Article

High Performance Polymers

High Performance Polymers
1–9

DOI: 10.1177/0954008319840404
journals.sagepub.com/home/hip
SAGE

Enhancing mode I and II interlaminar fracture toughness of carbon fiber-filled epoxy-based composites using both rice husk silica and silk fibroin electrospun nanofibers

Quang-Vu Bach[1], Cuong Manh Vu[2], Huong Thi Vu[3] and Dinh Duc Nguyen[4,5]

Abstract

In this study, we used both silk fibroin nanofibers (nSFs) and rice husk silica nanoparticles as epoxy (EP) resin reinforcement materials to improve the modes I and II interlaminar fracture toughness of EP-filled carbon fiber-based (CF/EP) composites. The nSFs were obtained by electrospinning, while the rice husk silica nanoparticles were obtained via acidic and thermal treatments. The results showed that the interfacial shear strength, G_{IC}, and G_{IIC} of the CF/EP composites improved by 25, 36, and 30%, respectively, by adding 0.2 wt% nSF and 20 wt% silica nanoparticles.

Keywords

Fracture toughness, rice husk silica nanoparticles, silk fibroin nanofibers, epoxy resin-filled carbon fiber-based composites, electrospinning, K_{IC}, mode i and mode ii interlaminar fracture toughness

Introduction

Owing to their high strength/density ratios, carbon fiber (CF)-filled polymeric matrix-based composite materials[1–6] are extensively used in aerospace, automotive, and marine applications. Both thermoplastic[7–9] and thermoset resins are used as the polymeric matrices for these composites.[10–14] Owing to their excellent specific tensile properties and wear resistance, CFs are widely used as the reinforcement material for the fabrication of advanced composites.[9] Thermoset resins such as epoxy (EP),[5,14] unsaturated polyester,[15] and vinyl ester[10] resins are commonly used for preparing CF-based composites. Among these, EP resin is the most widely used thermoset resin for industrial applications.[16–18] These resins exhibit excellent chemical resistance, excellent mechanical properties, compatibility with many reinforcement materials, and low shrinkage.[19] However, these resins suffer from low impact resistance or brittleness, which limits their use in high-performance applications.[16] EP resin-filled CF-based (CF/EP) composites show a mode I interlaminar fracture toughness (G_{IC}) of 80,300 kJ m^{-2}.[20] G_{IC} of these composited can be improved by modifying the EP resin matrix.[20] Additives such as liquid rubber,[21–23] thermoplastics,[24] nanomaterials,[25–28] and block copolymers[29–33] have been used for

[1] Sustainable Management of Natural Resources and Environment Research Group, Faculty of Environment and Labour Safety, Ton Duc Thang University, Ho Chi Minh City, Vietnam
[2] Faculty of Chemical-Physical Engineering, Le Quy Don Technical University, Hanoi, Vietnam
[3] AQP Research and Control Pharmaceuticals Joint Stock Company (AQP Pharma J.S.C), Dong Da, Hanoi, Vietnam
[4] Center for Advanced Chemistry, Institute of Research and Development, Duy Tan University, Da Nang, Vietnam
[5] Department of Environmental Energy Engineering, Kyonggi University, Suwon, South affKorea

Corresponding authors:
Quang-Vu Bach, Sustainable Management of Natural Resources and Environment Research Group, Faculty of Environment and Labour Safety, Ton Duc Thang University, Ho Chi Minh City, Vietnam.
Email: bachquangvu@tdtu.edu.vn

Cuong Manh Vu, Faculty of Chemical-Physical Engineering, Le Quy Don Technical University, 236 Hoang Quoc Viet, Hanoi, Vietnam.
Email: vumanhcuong309@gmail.com

Dinh Duc Nguyen, Center for Advanced Chemistry, Institute of Research and Development, Duy Tan University, Da Nang, Vietnam; Department of Environmental Energy and Engineering, Kyonggi University, Suwon 442-760, South Korea.
Email: nguyensyduc@gmail.com

enhancing the toughness of EP resin. Most of these additives are obtained from petroleum or are formed via chemical reactions. However, the growing concern for environmental protection has led to the use of environmentally friendly additives for the fabrication of composite materials.[34] Silk fibroin electrospun fibers (nSF) have gained immense attention as green additives for composite materials owing to their environmental friendliness and natural origin.[35,36] These fibers can be obtained by electrospinning silk fibroin solutions. These fibers have been used to improve the mode I interlaminar fracture toughness of CF-based composites.[37] Rice husk is an agricultural waste obtained from rice milling, and hence is cheap.[38] It has been reported that the silica component of rice husk can be used as an effective reinforcement material for various composites.[38,39] In addition, the use of rice husk silica can increase the cost-effectiveness and environmental friendliness of the composite fabrication process.

Both nSF[37] and rice husk silica[38] have been successfully used as EP resin reinforcement materials. For their application as the reinforcement materials for EP resin, rice husk-based silica nanoparticles and nSF are well blended with EP resin using a process homogenizer (15,000 r min^{-1}) and an ultrasonic homogenizer. The nSF and silica contents in these works were as low as 0.03–0.1 wt% and 0.03–0.1 phr, respectively. In this study, we used both nSF and rice husk silica nanoparticles as EP resin toughenners for the fabrication of CF/EP composites. The silica content used in this study was higher than that used in previous studies and was kept constant at 20 wt% to ensure the cost-effectiveness of the fabrication process, while the nSF content was varied from 0.1 wt% to 0.3 wt%. The composite materials were fabricated by the hand layup method, and their mode I and II interlaminar fracture toughness and morphology were investigated. The rheological testing, resin fracture toughness measurements, and morphology examinations of both the uncured and cured EP resin-based samples were carried out. The interaction between the CF and the EP resin matrices was evaluated using the interfacial shear strength (IFSS) testing method.

Experimental section

Materials

The bisphenol-A-based EP resin (DER 331) was purchased from Dow Chemical Company (Torrance, California, USA). The CFs were supplied by Toray (Japan). Methylhexahydrophthalic anhydride (MHHPA) and 1-methylimidazole (NMI) were purchased from Lindau Chemical (England) and BASF (Germany), respectively. Lithium bromide, sodium carbonate, formic acid, and methanol were purchased from Sigma-Aldrich (Tu Liem District, Ha Noi, Viet Nam). Silk cocoons were collected from a traditional craft village (Thai Binh province, Vietnam).

Fabrication of nSF and rice husk silica

The nSFs were fabricated using the method used in our previous study.[37] Silica nanoparticles were also extracted from rice husk using the method used in our previous study.[38,40]

Preparation of CF/EP composites

The silica loading of all the modified samples was 20 wt%, while the nSF content was varied from 0 wt% to 0.3 wt% depending upon the weight of EP. Homogeneous mixtures of silica and nSFs were embedded in the EP resin matrix by high-speed mechanical stirring at 15,000 r min^{-1} for 3 h followed by ultrasonication for another 4 h. These mixtures were cooled to room temperature before blending them with the MHHPA curing agent and NMI accelerator using a magnetic stirrer. The EP: MHHPA: NMI ratio was kept constant at 100: 87: 2.8 for all the samples. These mixtures were either directly cured in a steel mold or were used as matrices for the fabrication of carbon-based composites. Curing process was performed at 130°C for 1 h and at 150°C for another 1 h in a convection oven.[37] The fiber volume of the carbon-based composites was 50 $\pm$ 2%.

Characterization

The elemental compositions of the nSF and silica nanoparticles were examined using energy dispersive X-ray spectroscopy (EDS). The resin fracture toughness (K_{IC}) was calculated using the method used in our previous study[19] according to ASTM D5045-99. The notch tip was machined using a rotating saw, and the pre-crack of the specimens was generated by tapping a fresh razor blade placed in the notch. The fracture toughness tests were carried out at a cross-head speed of 10 mm min^{-1}. Each sample was tested at least five times and the average K_{IC} values were reported. K_{IC} values were calculated using the following equations

$$K_{IC} = \left(\frac{P_Q}{BW^{\frac{1}{2}}}\right) f(x) \quad (1)$$

with

$$f(x) = 6x^{\frac{1}{2}} \frac{[1.99 - x(1-x)(2.15 - 3.93x + 2.7x^2]}{(1+2x)(1-x)^{\frac{3}{2}}}$$

where P_Q is the critical load for crack propagation (kN), B is the specimen thickness (cm), W is the specimen width (cm), $f(x)$ is the nondimensional shape factor, a is the crack length (cm), and $x = a/W$. The value of a/W was varied from 0.45 to 0.55. The sample geometry for resin fracture toughness measurements is shown in Figure 1.

The rheological properties of the uncured resin were investigated using the procedure used in our previous study.[10]

In order to determine the IFSS of the samples, a detached single fiber was attached to a hard board using an adhesive and was then subjected to measurements using

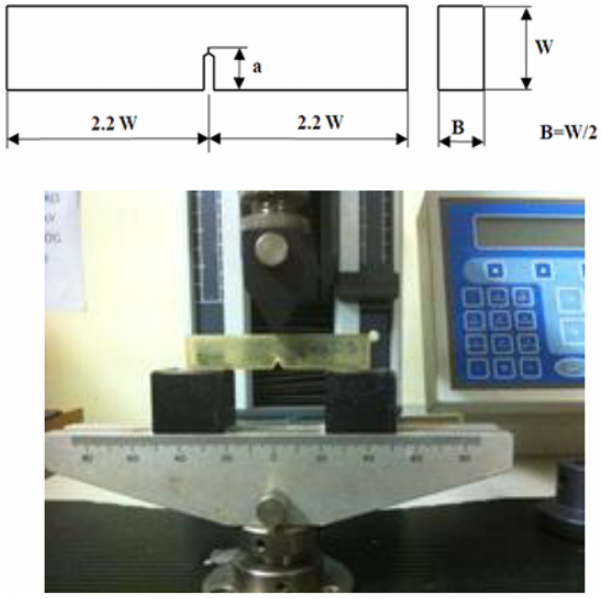

Figure 1. Fracture toughness test of resin samples.

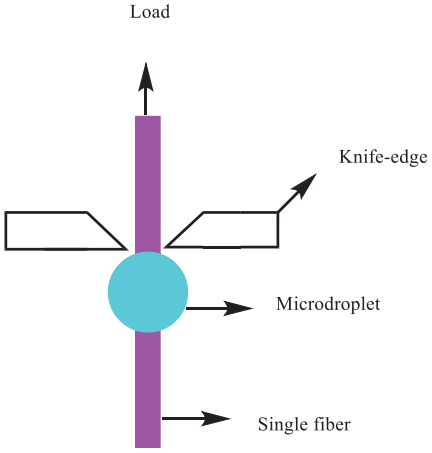

Figure 2. Schematic of the IFSS test. IFSS: interfacial shear strength.

a Model HM410 instrument (Shinjuku-Ku, Tokyo, Japan), as shown in Figure 2.[37]

The mode I interlaminar fracture toughness of the samples was evaluated using ASTM D5528-01.[20,41] The mode II interlaminar fracture toughness test (G_{IIC}) was carried out using the procedure used in our previous study.[37] The sample geometries for both mode I and II fracture toughness measurements are shown in Figure 3.

The morphologies of the rice husk silica nanoparticles, nFSs, and fractured surfaces were observed using scanning electron microscopy (SEM; JEOL JSM 6360, Japan).[37]

The appearance of nanomaterial in EP matrix was observed by a transmission electron microscope (TEM; JEM 1010-JEOL, Japan).

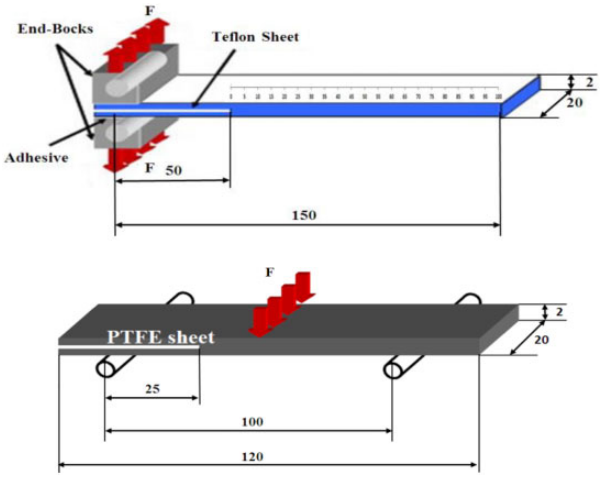

Figure 3. Mode I and II specimen geometry.

Results and discussions

Characterization of nSF and SiO_2

The nSF were obtained from electrospinning processing, and their morphology is shown in Figure 4.

The nSFs exhibited a web-like structure, in which many fibers were stacked up together. The diameter of these fibers varied from 30 nm to 80 nm. The strong interaction between these fibers can be attributed to hydrogen bonding and Van der Waals forces. High-speed mechanical stirring and ultrasonication were used to separate these fibers to obtain a homogeneous mixture with EP resin. The silica nanoparticles were extracted from rice husk, as shown in Figure 5.

Figure 5 shows that the silica nanoparticles were nearly spherical with a diameter of 20–60 nm. Agglomeration could also be observed because of the H-bonds between the particles. The elemental compositions of the nSF and rice husk silica nanoparticles are shown in Figure 6.

The nSF consisted of carbon, nitrogen, and oxygen (O). On the other hand, the rice husk silica nanoparticles consisted mainly of silicon and O. No carbon and metal impurities were detected in the EDS spectrum of the silica nanoparticles, indicating a complete combustion of the rice husk.

Rheological properties of the uncured samples

The rheological properties of uncured matrices affect the processing and properties of composite materials. In general, high-viscosity resins can hardly permeate nSFs. Low-viscosity resins, on the other hand, can easily penetrate such fibers. The relationship between the shear rate and shear stress and between shear rate and viscosity of the composites is shown in Figure 7.

It can be observed from Figure 7(a) that all the uncured EP resin-based mixtures exhibited a linear shear stress–shear rate relationship. The pristine uncured EP resin showed Newtonian characteristics with no shear thinning

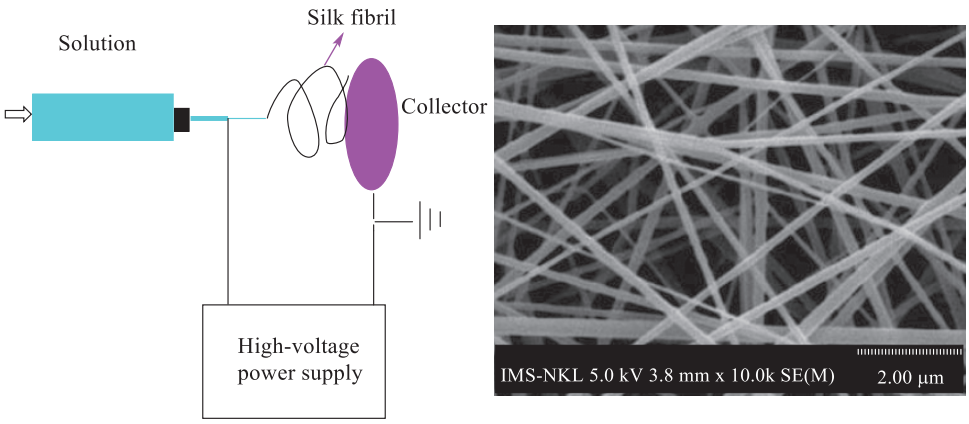

Figure 4. Electrospinning processing and morphology of nSF.

Figure 5. Rice husk in acidic solution, silica rice husk, and scanning electron microscopic image of silica nanoparticles.

behavior. The EP/20 silica (SiO_2) and EP/20 SiO_2/0.x nSF ($x = 13$) resins, on the other hand, exhibited non-Newtonian characteristics or a pseudo-plastic behavior. This pseudo-plasticity occurred at lower shear rates because of the significant increase in the rigidity of the systems through the formation of silica and nSF agglomerates. Initially, weak dipoles such as Van der Waal's interactions or H-bonding between the SiO_2 and nSF agglomerates hindered the alignment of the EP chains. With an increase in the shear rate, either these interactions weakened or the agglomerates decomposed and the EP chains aligned rapidly in the direction of the increasing shear rate, resulting in a shear-thinning behavior. This was confirmed by the viscosity versus shear rate graph shown in Figure 7(b). With an increase in the nSF loading, the viscosity of the EP resin increased gradually irrespective of the shear rate because of the nSF-induced increase in their rigidity. The viscosity of the uncured EP resin was found to be independent of the shear rate, indicating a Newtonian flow. The viscosity of the EP resin matrices with SiO_2/nSF

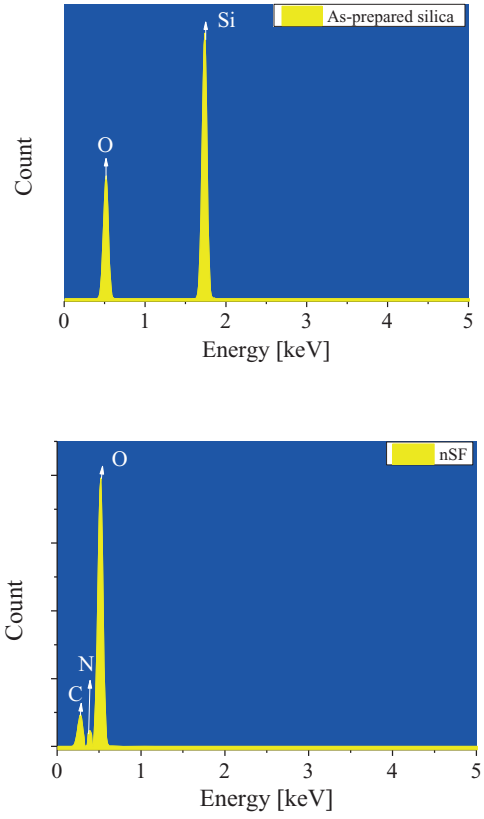

Figure 6. EDS spectra of nSFs and rice husk-based silica nanoparticles. EDS: energy dispersive X-ray spectroscopy.

(20/0; 20/0.1; 20/0.2; 20/0.3), on the other hand, decreased with an increase in the shear rate from 100 s^{-1} and 250 s^{-1}. However, the viscosity saturated at higher shear rates. This is because an increase in the nSF content increased the heterogeneity of the system, which resisted the flow and alignment of the polymeric chains.

Resin fracture toughness

The resin fracture toughness of the cured EP resins with different SiO_2/nSF ratios (0/0; 20/0; 20/0.1; 20/0.2; 20/0.3) was determined using the three-point bending method. In order to prevent the viscoelastic characteristics of EP resin, the cross-head speed was maintained at 10 mm min^{-1}. Figure 8 shows the effect of the SiO_2/nSF ratio on K_{IC} values of the EP resin matrices.

From Figure 8, it can be observed that K_{IC} value of the EP resin matrices increased with the incorporation of SiO_2 and the nSF. K_{IC} of EP resin increased significantly from 0.638 MPa·$m^{½}$ at SiO_2/nSF = 0/0 to 1.215 MPa·$m^{½}$ at SiO_2/nSF = 20/0.2. The fracture surfaces of the EP resin samples were examined by SEM (Figure 9) in order to verify K_{IC} results.

The virgin EP resin showed a smooth fracture surface Figure 9(a). This indicates that the energy required for crack growth was low in this case, and the cracks could propagate easily. The addition of SiO_2/nSF increased the

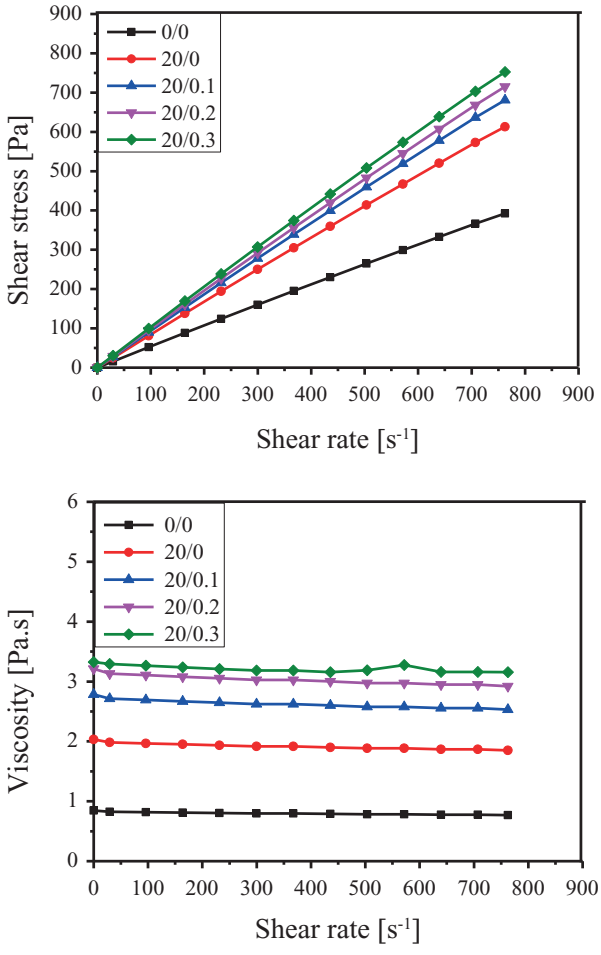

Figure 7. Effect of the SiO_2/nSF ratio on the rheological properties of EP. SiO_2: silica; EP: epoxy.

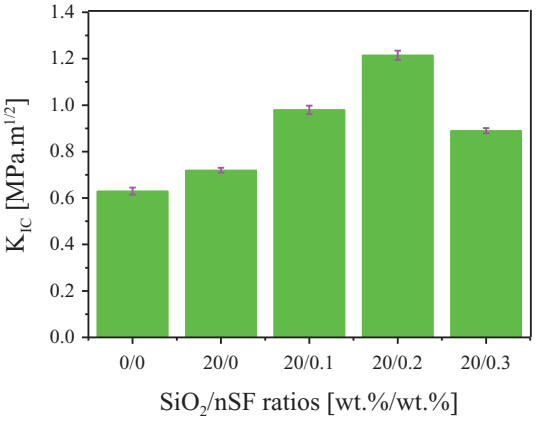

Figure 8. Effect of the SiO_2/nSF ratio on the fracture toughness of EP (K_{IC}). SiO_2: silica; EP: epoxy.

roughness of the fracture surface of EP resin. This indicates that, in these samples, crack propagation was slow and more energy was required for crack growth. This can be attributed to the nanofiber bridging of the cracks, as shown in Figure 9(b) and (c).

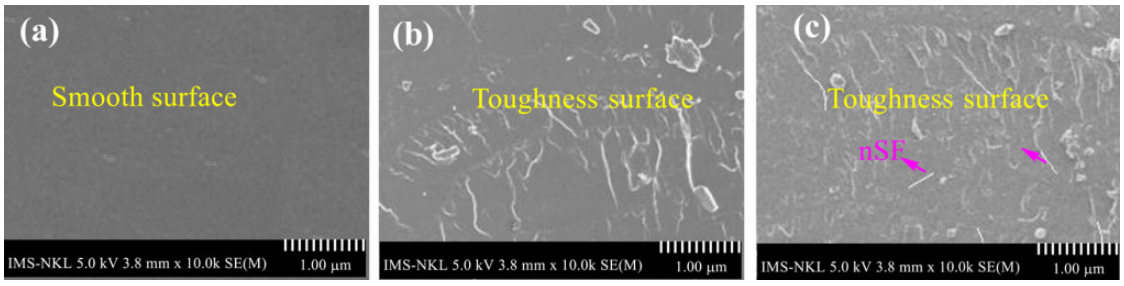

Figure 9. Scanning electron microscopic images of the fracture surface of (a) pristine sample, (b) EP with 20 wt% SiO_2, and (c) EP with 20 wt% SiO_2 and 0.2 wt% nSF. EP: epoxy; SiO_2: silica.

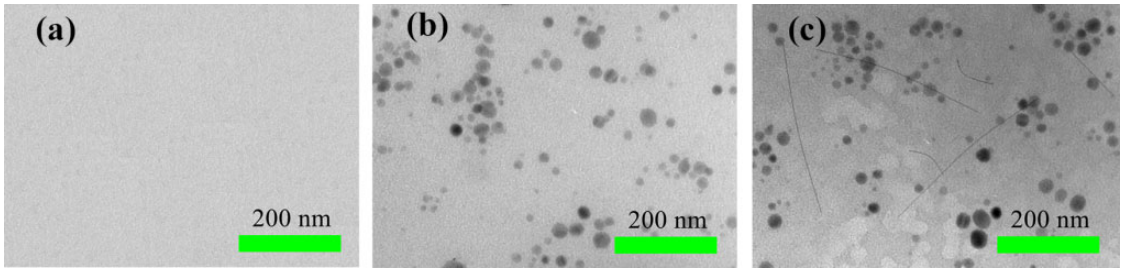

Figure 10. Transmission electron microscopic images of (a) pristine sample, (b) EP with 20 wt% SiO_2, and (c) EP with 20 wt% SiO_2 and 0.2 wt% nSF. EP: epoxy; SiO_2: silica.

TEM images (Figure 10) of the pristine and modified cured EP resin samples were also obtained to confirm the presence of the reinforcement materials in them. The cured virgin EP resin showed no reinforcement. The modified EP resin samples showed the presence of both the silica nanoparticles and nSFs.

Microdroplet test

The interface between CF and EP resin significantly affects the properties of CF/EP composites. We carried out IFSS testing to examine this interface. The effect of the SiO_2/nSF ratio on the force, displacement, and average IFSS values of the composites is shown in Figure 11.

From Figure 11, it can be observed that the maximum force increased with an increase in the nSF content. However, the displacement decreased with an increase in the nSF content. This can be attributed to the presence of H-bonds between SiO_2 and the nSF with CF. The average IFSS values of the samples were calculated from five experimental testing values. The average IFSS value of the composites increased with an increase in the nSF content. The average IFSS value of EP resin increased significantly (by 25%) from 63.15 MPa at SiO_2/nSF 0/0 to 79.68 MPa at SiO_2/nSF = 20/0.2. Both SiO_2 and the nSFs contributed to the improvement of the interphase between the CF and EP resin.

Mode I and II interlaminar fracture toughness test

Figure 12 shows the effect of the SiO_2/nSF ratio on the mode I interlaminar fracture toughness of the composites.

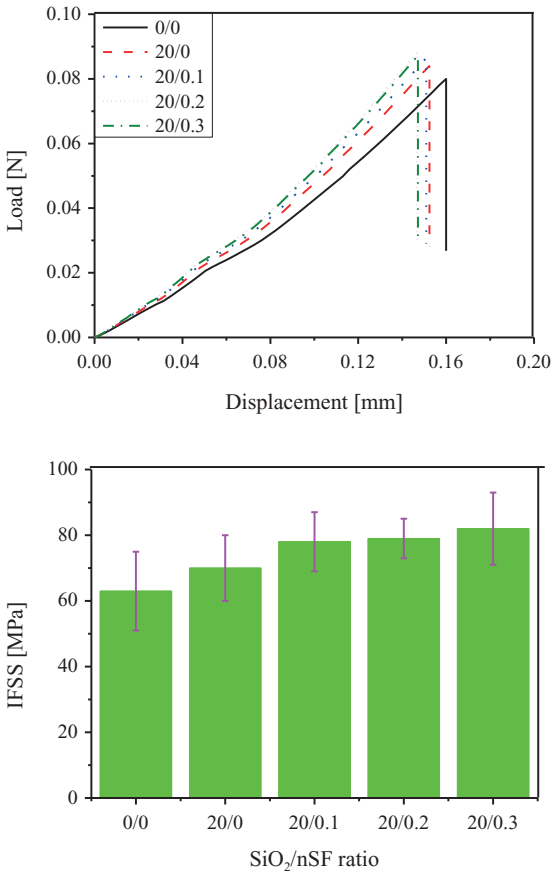

Figure 11. Load, displacement, and IFSS values of composites with different SiO_2/nSF ratios. IFSS: interfacial shear strength; SiO_2: silica.

The average G_{IC} and G_{IP} values of the pristine sample were found to be 602.34 and 723.15 J m^{-2}, respectively. From Figure 12, it can be observed that the G_{IC} and G_{IP} values increased with an increase in the nSF content. The SiO_2/nSF ratio of about 20/0.2 was found to be optimum. G_{IC} value of EP resin increased (by 37%) from 389.82 kJ m^{-2} at SiO_2/nSF = 0/0 to 536.68 kJ m^{-2} at SiO_2/nSF = 20/0.2. G_{IP} value of EP resin increased (by 41%) from 401.38 kJ m^{-2} at SiO_2/nSF = 0/0 to 568.32 kJ m^{-2} at SiO_2/nSF = 20/0.2. Thus, the presence of the additives in the EP resin matrices improved the fracture toughness of the CF-based composites. The improvement in the mode I interlaminar fracture toughness of the composites can be attributed to mechanisms such as crack deflection (tiling or twisting motion around the fibers), debonding between the CF and the resin, pullout (extraction of the fibers from the resin), and fiber bridging. However, it was difficult to determine the dominant mechanism. Figure 13 shows the morphologies of the mode I interlaminar fracture surfaces of the modified and unmodified CF-based composites.

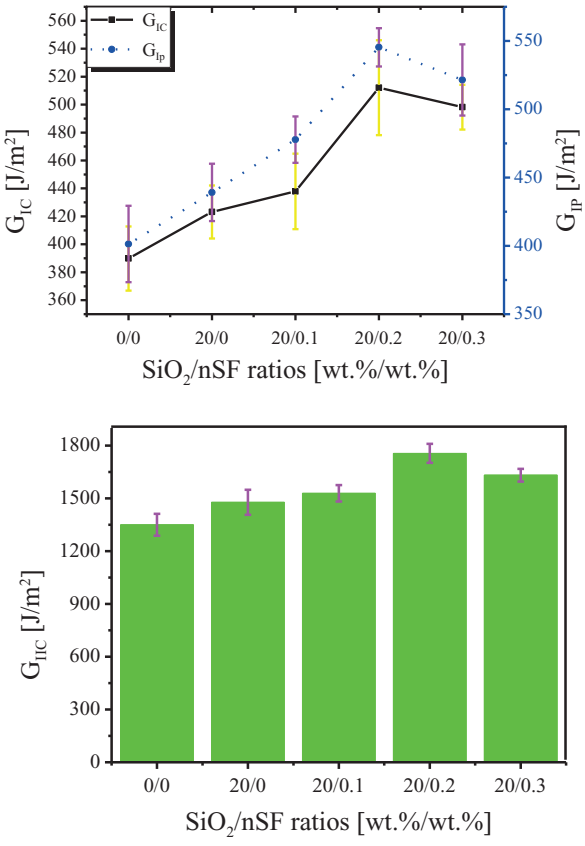

Figure 12. Effect of the SiO_2/nSF ratio on the G_{IC} and G_{IIC} values of the composites. SiO_2: silica.

The unmodified composite showed a smooth surface because of its low crack development energy. On the other hand, the modified composites showed a fracture surface with fibers pulling out from the resin matrix. This indicates that the energy required for crack growth was high in the modified composites.

In the end notch flexure test, the specimen was loaded in a three-point flexural fixture, as shown in Figure 3. Figure 12 also shows the interlaminar fracture toughness of the composites as a function the SiO_2/nSF ratio. These results were consistent with the mode I and II interlaminar fracture toughness results. The critical energy release (G_{IIC}) of the CF-based composite increased (by 30%) from 1350 kJ m^{-2} at SiO_2/nSF = 0/0 to 1756 kJ m^{-2} at SiO_2/nSF = 20/0.2. It should be noted that energy-dissipating mechanisms such as fiber matrix de-bonding, fiber pullout, fiber bridging, and fracturing of the matrix and fibers increase the fracture toughness of CF/EP composites.

Conclusions

In this study, the effect of the addition of rice husk silica nanoparticles and nSF on the mode I and II interlaminar fracture toughness of CF/EP composites was investigated. The silica nanoparticles were extracted from rice husk, and the nSFs were obtained by electrospinning. The uncured pristine EP resin exhibited Newtonian characteristics, while the modified uncured resins showed non-Newtonian characteristics. At SiO_2/nSF = 20/0.2, the mode

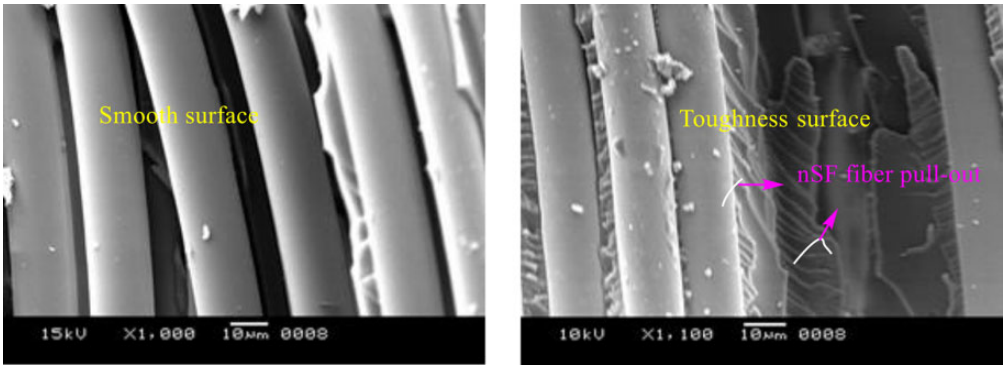

Figure 13. Fracture surface of the (a) unmodified and (b) modified CF/EP composite. CF: carbon fiber; EP: epoxy.

I and II fracture toughness of the CF/EP composite increased by about 36 and 30%, respectively. The fracture surfaces of the modified composites were rougher and tougher than that of the pristine sample. These composites can be used for high-performance applications.

Declaration of conflicting interests

The author(s) declared no potential conflicts of interest with respect to the research, authorship, and/or publication of this article.

Funding

The author(s) disclosed receipt of the following financial support for the research, authorship, and/or publication of this article: This research was funded by Vietnam National Foundation for Science and Technology Development (NAFOSTED) under grant number 104.02-2017.15 (for Cuong Manh Vu) and by grants from the National Research Foundation (NRF) of Korea (grant no. NRF-2017R1D1A1B03035442).

ORCID iD

Cuong Manh Vu https://orcid.org/0000-0001-8986-1015

References

1. Gabr MH, Okumura W, Ueda H, et al. Mechanical and thermal properties of carbon fiber/polypropylene composite filled with nano-clay. *Compos B: Eng* 2015; **69**: 94–100.
2. Ashori A, Menbari S and Bahrami R. Mechanical and thermo-mechanical properties of short carbon fiber reinforced polypropylene composites using exfoliated graphene nanoplatelets coating. *J Ind Eng Chem* 2016; **38**: 37–42.
3. Luo W, Zhang B, Zou H, et al. Enhanced interfacial adhesion between polypropylene and carbon fiber by graphene oxide/polyethyleneimine coating. *J Ind Eng Chem* 2017; **51**: 129–139.
4. Unterweger C, Duchoslav J, Stifter D, et al. Characterization of carbon fiber surfaces and their impact on the mechanical properties of short carbon fiber reinforced polypropylene composites. *Compos Sci Tech* 2015; **108**: 41–47.
5. Xiao C, Tan Y, Wang X, et al. Study on interfacial and mechanical improvement of carbon fiber/epoxy composites by depositing multi-walled carbon nanotubes on fibers. *Chem Phys Lett* 2018; **703**: 8–16.
6. Ma Y, Yan C, Xu H, et al. Enhanced interfacial properties of carbon fiber reinforced polyamide 6 composites by grafting graphene oxide onto fiber surface. *Appl Surf Sci* 2018; **452**: 286–298.
7. Yamamoto T, Uematsu K and Yabushita S. Enhancement of mechanical properties of carbon fiber reinforced thermoplastic using colloidal techniques. *Procedia Manuf* 2018; **15**: 1738–1745.
8. Kim BJ, Cha SH and Park YB. Ultra-high-speed processing of nanomaterial-reinforced woven carbon fiber/polyamide 6 composites using reactive thermoplastic resin transfer molding. *Compos B: Eng* 2018; **143**: 36–46.
9. Yao SS, Jin FL, Rhee KY, et al. Recent advances in carbon-fiber-reinforced thermoplastic composites: a review. *Compos B: Eng* 2018; **142**: 241–250.
10. Nguyen LT, Vu CM, Phuc BT, et al. Simultaneous effects of silanized coal fly ash and nano/micro glass fiber on fracture toughness and mechanical properties of carbon fiber reinforced vinyl ester resin composites. *Polym Eng Sci* 2018; **59**: 584–591. DOI: 10.1002/pen.24973.
11. Yourdkhani M, Liu W, Baril-Gosselin S, et al. Carbon nanotube-reinforced carbon fibre-epoxy composites manufactured by resin film infusion. *Compos Sci Tech* 2018; **166**: 169–175.
12. Wang Q, Ning H, Vaidya U, et al. Development of a carbonization-in-nitrogen method for measuring the fiber content of carbon fiber reinforced thermoset composites. *Compos A: Appl Sci Manuf* 2015; **73**: 80–84.
13. Mgbemena CO, Li D, Lin MF, et al. Accelerated microwave curing of fibre-reinforced thermoset polymer composites for structural applications: a review of scientific challenges. *Compos A: Appl Sci Manuf* 2018; **115**: 88–103.
14. Zhang Z, Wang C, Huang G, et al. Thermal degradation behaviors and reaction mechanism of carbon fibre-epoxy composite from hydrogen tank by TG-FTIR. *J Hazard Mater* 2018; **357**: 73–80.
15. Jiang D, Xing L, Liu L, et al. Interfacially reinforced unsaturated polyester composites by chemically grafting different functional POSS onto carbon fibers. *J Mater Chem A* 2014; **2**: 18293–18303.
16. Vu CM, Sinh LH, Nguyen DD, et al. Simultaneous improvement of the fracture toughness and mechanical characteristics of amine-functionalized nano/micro glass fibril-reinforced epoxy resin. *Polym Test* 2018; **71**: 200–208.
17. Vu CM, Nguyen DD, Sinh LH, et al. Environmentally benign green composites based on epoxy resin/bacterial cellulose reinforced glass fiber: fabrication and mechanical characteristics. *Polym Test* 2017; **61**: 150–161.
18. Vu CM, Nguyen TV, Nguyen LT, et al. Fabrication of adduct filled glass fiber/epoxy resin laminate composites and their physical characteristics. *Polym Bull* 2016; **73**: 1373–1391.
19. Vu CM, Sinh LH, Choi HJ, et al. Effect of micro/nano white bamboo fibrils on physical characteristics of epoxy resin reinforced composites. *Cellulose* 2017; **24**: 5475–5486.
20. Vu CM, Nguyen LT, Nguyen TV, et al. Effect of additive-added epoxy on mechanical and dielectric characteristics of glass fiber reinforced epoxy composites. *Polym Kor* 2014; **38**: 726–734.
21. Xiao X, Shiqiao G, Dongmei Z, et al. Mechanical behavior of liquid nitrile rubber-modified epoxy resin: experiments, constitutive model and application. *Inter J Mechan Sci* 2019; **151**: 46–60.
22. Ricciardi MR, Papa I, Langella A, et al. Mechanical properties of glass fibre composites based on nitrile rubber toughened modified epoxy resin. *Compos B: Eng* 2018; **139**: 259–267.

23. Wang L, Tan Y, Wang H, et al. Investigation on fracture behavior and mechanisms of DGEBF toughened by CTBN. *Chem Phys Lett* 2018; **699**: 14–21.
24. Shin H, Kim B, Han JG, et al. Fracture toughness enhancement of thermoplastic/epoxy blends by the plastic yield of toughening agents: a multiscale analysis. *Compos Sci Tech* 2017; **145**: 173–180.
25. Abidin MS, Herceg T, Greenhalgh ES, et al. Enhanced fracture toughness of hierarchical carbon nanotube reinforced carbon fibre epoxy composites with engineered matrix microstructure. *Compos Sci Tech* 2019; **170**: 85–92.
26. Quan D, Urdániz JL and Ivanković A. Enhancing mode-I and mode-II fracture toughness of epoxy and carbon fibre reinforced epoxy composites using multi-walled carbon nanotubes. *Mater Des* 2018; **143**: 81–92.
27. Cha J, Jun GH, Park JK, et al. Improvement of modulus, strength and fracture toughness of CNT/epoxy nanocomposites through the functionalization of carbon nanotubes. *Compos B: Eng* 2017; **129**: 169–179.
28. Adak NC, Chhetri S, Kuila T, et al. Effects of hydrazine reduced graphene oxide on the inter-laminar fracture toughness of woven carbon fiber/epoxy composite. *Compos B: Eng* 2018; **149**: 22–30.
29. Heng Z, Zhang X, Chen Y, et al. In-situ construction of "octopus"-like nanostructure to achieve high performance epoxy thermosets. *Chem Eng J* 2019; **360**: 542–552.
30. Heng Z, Zeng Z, Zhang B, et al. Enhancing mechanical performance of epoxy thermosets via designing a block copolymer to self-organize into "core–shell" nanostructure. *RSC Adv* 2016; **6**: 77030–77036.
31. Li M, Heng Z, Chen Y, et al. High toughness induced by wormlike-nanostructure in epoxy thermoset containing amphiphilic PDMS–PCL block copolymers. *Ind Eng Chem Res* 2018; **57**: 13036–13047.
32. Dean JM, Lipic PM, Grubbs RB, et al. Micellar structure and mechanical properties of block copolymer-modified epoxies. *J Polym Sci B: Polym Phys* 2001; **39**: 2996–3010.
33. Liu JD, Sue HJ, Thompson ZJ, et al. Nanocavitation in self-assembled amphiphilic block copolymer-modified epoxy. *Macromol* 2008; **41**: 7616–7624.
34. Vu CM, Nguyen DD, Sinh LH, et al. Micro-fibril cellulose as a filler for glass fiber reinforced unsaturated polyester composites: fabrication and mechanical characteristics. *Macromol Res* 2018; **26**: 54–60.
35. Cervantes SA, Pagán A, Martínez JG, et al. Electrospun silk fibroin scaffolds coated with reduced graphene promote neurite outgrowth of PC-12 cells under electrical stimulation. *Mater Sci Eng: C* 2017; **79**: 315–325.
36. Ghalei S, Nourmohammadi J, Solouk A, et al. Enhanced cellular response elicited by addition of amniotic fluid to alginate hydrogel-electrospun silk fibroin fibers for potential wound dressing application. *Colloid Surf B: Biointerf* 2018; **172**: 82–89.
37. Vu CM and Choi HJ. Enhancement of interlaminar fracture toughness of carbon fiber/epoxy composites using silk fibroin electrospun nanofibers. *J Polym Plast Tech Eng* 2016; **55**: 1048–1056.
38. Pham TD, Vu CM and Choi HJ. Enhanced fracture toughness and mechanical properties of epoxy resin with rice husk-based nano-silica. *Polym Sci Ser A* 2017; **59**: 437–444.
39. Battegazzore D, Bocchini S, Alongi J, et al. Rice husk as bio-source of silica: preparation and characterization of PLA–silica bio-composites. *RSC Adv* 2014; **4**: 54703–54712.
40. Kwon SH, Park IH, Vu CM, et al. Fabrication and electro-responsive electrorheological characteristics of rice husk-based nanosilica suspension. *J Taiwan Inst Chem Eng* 2018; **95**: 432–437. DOI: 10.1016/j.jtice.2018.08.018.
41. Phong NT, Gabr MH, Okubo K, et al. Enhancement of mechanical properties of carbon fabric/epoxy composites using micro/nano-sized bamboo fibrils. *Mater Des* 2013; **47**: 624–632.